

## Supporting Information to

### Anomalous Behavior of the Homogeneous Ice Nucleation Rate in “No-Man’s Land”

#### Authors

Hartawan Laksmono, Trevor A. McQueen, Jonas A. Sellberg, N. Duane Loh, Congcong Huang, Daniel Schlesinger, Raymond G. Sierra, Christina Y. Hampton, Dennis Nordlund, Martin Beye, Andrew V. Martin, Anton Barty, M. Marvin Seibert, Marc Messerschmidt, Garth J. Williams, Sébastien Boutet, Katrin Amann-Winkel, Thomas Loerting, Lars G. M. Pettersson, Michael J. Bogan, and Anders Nilsson

#### Classical nucleation theory (CNT).

According to CNT,<sup>1-4</sup> the homogeneous ice nucleation rate at which critical nuclei appear within a supercooled liquid can be expressed by<sup>1-7</sup>

$$J = J_0 \exp\left(-\frac{\Delta F^*}{kT}\right),$$

where  $J_0$  is the temperature-dependent pre-exponential factor, and  $\Delta F^*$  is the Gibbs free energy barrier to form a critical nucleus from the liquid. Assuming that the molecular jump across the solid-liquid interface can be modeled based on viscous flow in the liquid,<sup>8</sup> we follow Chusak and Bartell<sup>6</sup> and represent the pre-exponential factor by

$$J_0 = 16 \left(\frac{3\pi}{4}\right)^{1/3} \left(\frac{\sigma_{sl}}{kT}\right)^{1/2} \frac{D}{(\nu_{ms})^{4/3}}$$

where  $\sigma_{sl}$  is the solid-liquid water interfacial free energy,  $k$  is the Boltzmann constant,  $D$  is the liquid water diffusivity, and  $\nu_{ms}$  is the ice molecular volume. The liquid diffusivity can be represented by

$$D = D_0 \exp\left(-\frac{E_D}{kT}\right),$$

where  $D_0$  is the pre-exponential factor, and  $E_D$  is the activation energy for diffusion in the liquid. We assume  $E_D$  is temperature dependent. In the CNT formalism,  $E_D$  also represents the activation energy ( $\Delta f^*$ ) for water molecules to jump across the solid-liquid interface.<sup>9</sup> Thus, there are two barriers to ice nucleation where  $\Delta F^*$  describes the thermodynamic barrier while  $\Delta f^*$  represents the kinetic barrier. Also within CNT, the thermodynamic barrier is given by<sup>3</sup>

$$\Delta F^* = \frac{16\pi\sigma_{sl}^3\nu_{ms}^2}{3(\Delta\mu_{sl})^2},$$

where  $\Delta\mu_{sl}$  is the difference in chemical potential between the solid and liquid phases evaluated at the pressure and temperature of the liquid phase. Thus  $\Delta\mu_{sl}$  can be evaluated from<sup>3</sup>

$$\Delta\mu_{sl} = \Delta\mu_{sl,0} + \Delta\mu_{sl,p},$$

where  $\Delta\mu_{sl,0}$  is calculated at a reference pressure and  $\Delta\mu_{sl,p}$  accounts for the chemical potential difference at the reference pressure and the liquid pressure. We calculated  $\Delta\mu_{sl,0}$  by using  $\Delta\mu_{sl,0} = -kT \ln(p_{e,l}/p_{e,s})$  where  $p_{e,l}$  and  $p_{e,s}$  are the equilibrium vapor pressures of the liquid and crystalline solid phases, respectively. The  $\Delta\mu_{sl,p}$  can be approximated by<sup>3</sup>

$$\Delta\mu_{sl,p} = (p_l - p_{e,s})\nu_{ms} - (p_l - p_{e,l})\frac{\nu_{ml}(p_l) + \nu_{ml}(p_{e,l})}{2},$$

where  $v_{ml}(p_l)$  and  $v_{ml}(p_{e,l})$  are the molecular volumes of liquid water at pressure  $p_l$  and  $p_{e,l}$ , respectively. However, the  $\Delta\mu_{s,l,p}$  is negligible relative to the  $\Delta\mu_{s,l,0}$  for droplets larger than roughly one  $\mu\text{m}$  in diameter because the internal pressure due to the Young-Laplace effect is relatively small.<sup>3</sup> Finally, we assume ice to nucleate as cubic ice following the results of several authors.<sup>7,10,11</sup>

### **Crystallization time may represent nucleation and growth at lowest temperature of $\sim 227\text{ K}$**

With an estimated critical ice nucleus diameter of  $\sim 2.5\text{ nm}$  and a growth rate of  $\sim 1 \times 10^8\text{ nm/s}$  at  $\sim 232\text{ K}$  (the growth rate lower limit in our analysis assuming the observed growth rate of  $\sim 3 \times 10^8\text{ nm/s}$  at  $238\text{ K}$ <sup>12</sup> scales with the decrease in diffusivity as temperature decreases), it takes  $\sim 2\ \mu\text{s}$  for the ice nucleus to grow to a distinguishable size and  $\sim 435\ \mu\text{s}$  to completely freeze the  $12\ \mu\text{m}$  droplet. Both are much faster than  $\sim 8,500\ \mu\text{s}$ , which is the estimated time to form a new nucleus within the droplet (approximated by  $1/JV_{\text{drop}}$ , where  $J \sim 10^{11}\text{ cm}^{-3}\text{s}^{-1}$  at  $\sim 232\text{ K}$ ). At the lowest temperature of  $\sim 227\text{ K}$  and an estimated growth rate of  $\sim 5 \times 10^5\text{ nm/s}$ , the time for the ice nucleus to grow to a distinguishable size ( $\sim 486\ \mu\text{s}$ ) is slightly longer than the time to form a new ice nucleus ( $\sim 405\ \mu\text{s}$ , with  $J \sim 10^{13}\text{ cm}^{-3}\text{s}^{-1}$  at  $\sim 227\text{ K}$ ). At this temperature, however, complete crystallization of the droplet requires much longer times ( $\sim 10^5\ \mu\text{s}$ ) than to form another nucleus. Thus, we note that the crystallization times may represent a combination of nucleation and growth at the lowest temperature of  $\sim 227\text{ K}$ .

### **Nucleation rate sensitivity to increased pressure according to CNT.**

Recently, a pressure-dependent CNT has been formulated to include the pressure dependence in the form of chemical potential differences that primarily alter the overall thermodynamic barrier to nucleation ( $\Delta F^*$ ).<sup>3</sup> In this formulation, an increase in pressure decreases the nucleation rate (Fig. S1) due to higher  $\Delta F^*$  at higher pressure (Fig. S2). For example, increasing the pressure from 0.1 MPa (black solid line in Fig. S1) to 50 MPa (gray solid line in Fig. S1), equivalent to reducing droplet diameter from a few micrometers to a few nanometers, decreases the nucleation rate significantly at temperatures above 200 K. This is because the pressure contribution to the thermodynamic energy barrier ( $\Delta F_p^*$ ) (assuming  $\Delta\mu_{sl} = \Delta\mu_{sl,p}$ , see Experimental Section) is significant at 50 MPa (gray solid line with plus symbol in Fig. S2) and contributes up to  $\sim 17\%$  of  $\Delta F^*$  (gray solid line in Fig. S2) at higher temperature, but the  $\Delta F_p^*$  is negligible below 200 K. In contrast  $\Delta F_p^*$  at 0.1 MPa (black solid line with plus symbol in Fig. S2) is negligible over the same temperature range. However, this analysis ignores the pressure effect on liquid diffusivity ( $D$ ). The  $D$  may affect the nucleation rate significantly within the “no-man’s land” by altering the kinetic barrier to nucleation ( $\Delta f^*$ ). When a CNT analysis is performed to include the effect of pressure on the  $D$  alone, a pressure increase of 50 MPa increases the nucleation rate at lower temperature (compare gray solid line versus gray dashed line in Fig. S1). This is due to a significant decrease in the  $\Delta f^*$  at lower temperature (compare black solid line against gray dashed line in Fig S3). In this illustration, we assumed that an extrapolation of the  $D_{VFT}$  fitted to  $D$  data above  $T_H$ <sup>13</sup> describes the  $D$  within “no-man’s land”. Figure S4 shows that the  $D_{VFT}$  at 50 MPa (black solid line) decreases more rapidly than the  $D_{VFT}$  at 0.1 MPa (gray dashed line) with decreasing temperature. When the pressure dependence of both barriers are accounted for, the pressure increase lowers the nucleation rate at temperatures above 220 K, but increases the nucleation rate at temperatures below 220 K (compare black solid line to gray dashed line in Fig. S1). Thus, the pressure effect on both  $\Delta F^*$  and  $\Delta f^*$  needs to be considered when comparing ice nucleation rate results from various experiments over a wide range of temperatures and pressures, particularly below 235 K.

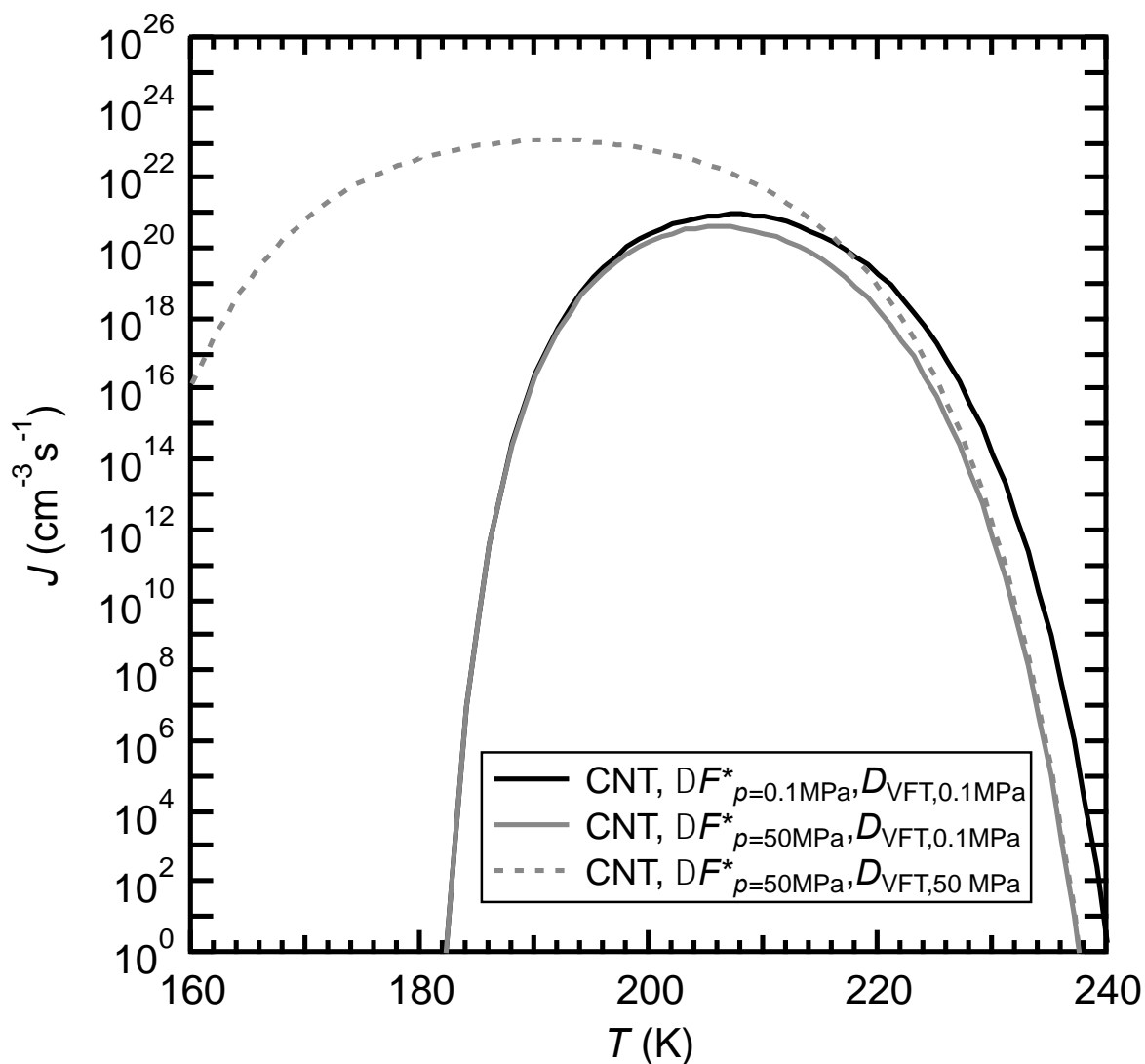


**Figure S1.** The nucleation rate ( $J$ ) is sensitive to both temperature and pressure according to a pressure-dependent CNT analysis. Increasing pressure from 0.1 MPa (black solid line) to 50 MPa (gray solid line) decreases  $J$  at higher temperature when diffusivity ( $D$ ) is assumed to be pressure independent. In contrast, a 50 MPa increase in pressure increases  $J$  at lower temperature assuming the pressure change only affects the  $D$  (see gray solid and dashed lines). Overall, the pressure increase from 0.1 MPa (black solid line) to 50 MPa (gray dashed line) causes  $J$  to decrease and increase for temperatures above and below 220 K, respectively.

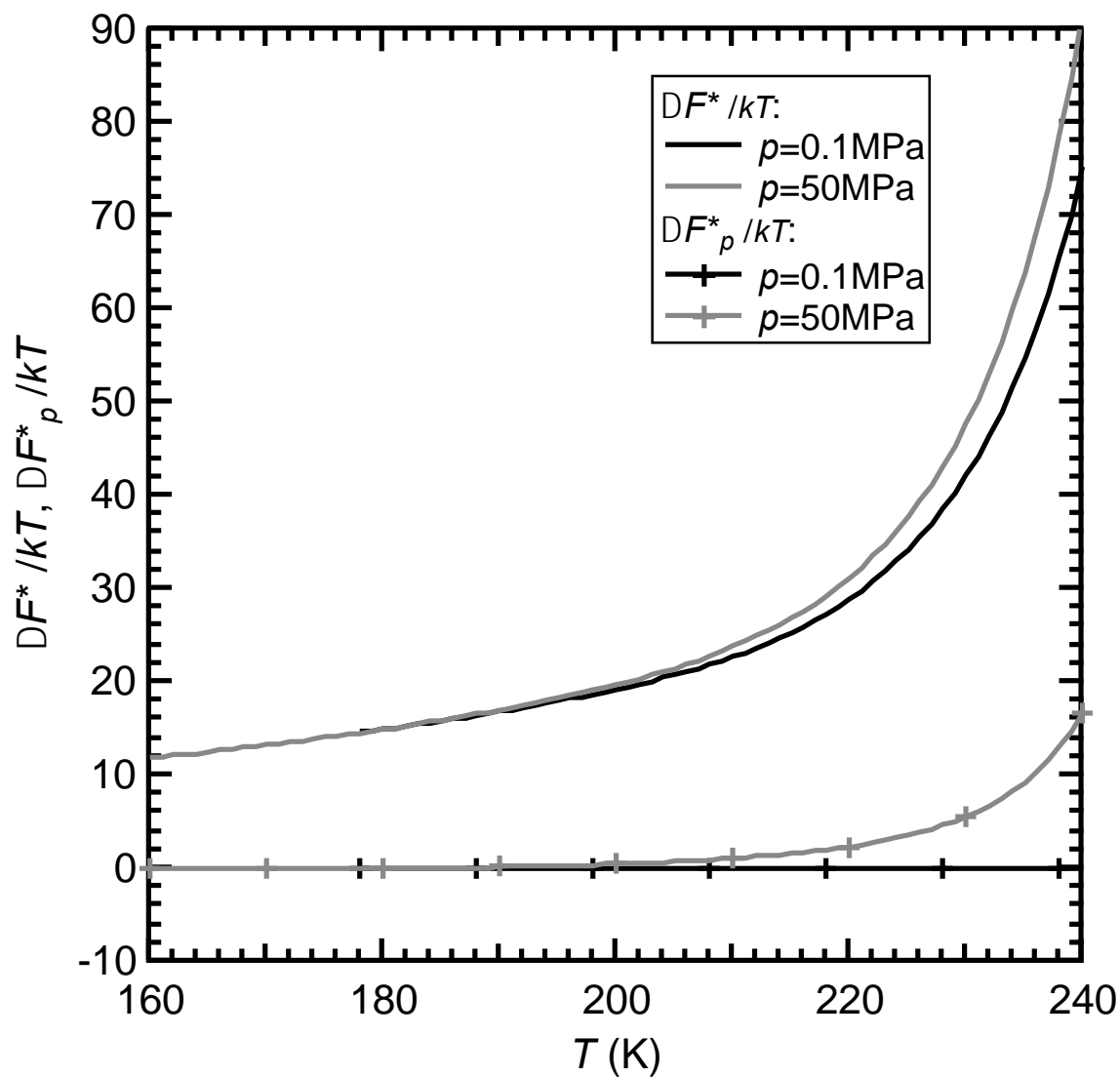


**Figure S2.** The pressure contribution to the thermodynamic energy barrier ( $\Delta F_p^*$ ) between 160 K and 240 K. The  $\Delta F_p^*$  at 0.1 MPa (black solid line with plus marker) is negligible. Likewise, the  $\Delta F_p^*$  at 50 MPa (gray solid line with plus marker) is negligible below 200 K but it increases significantly with increasing temperature.

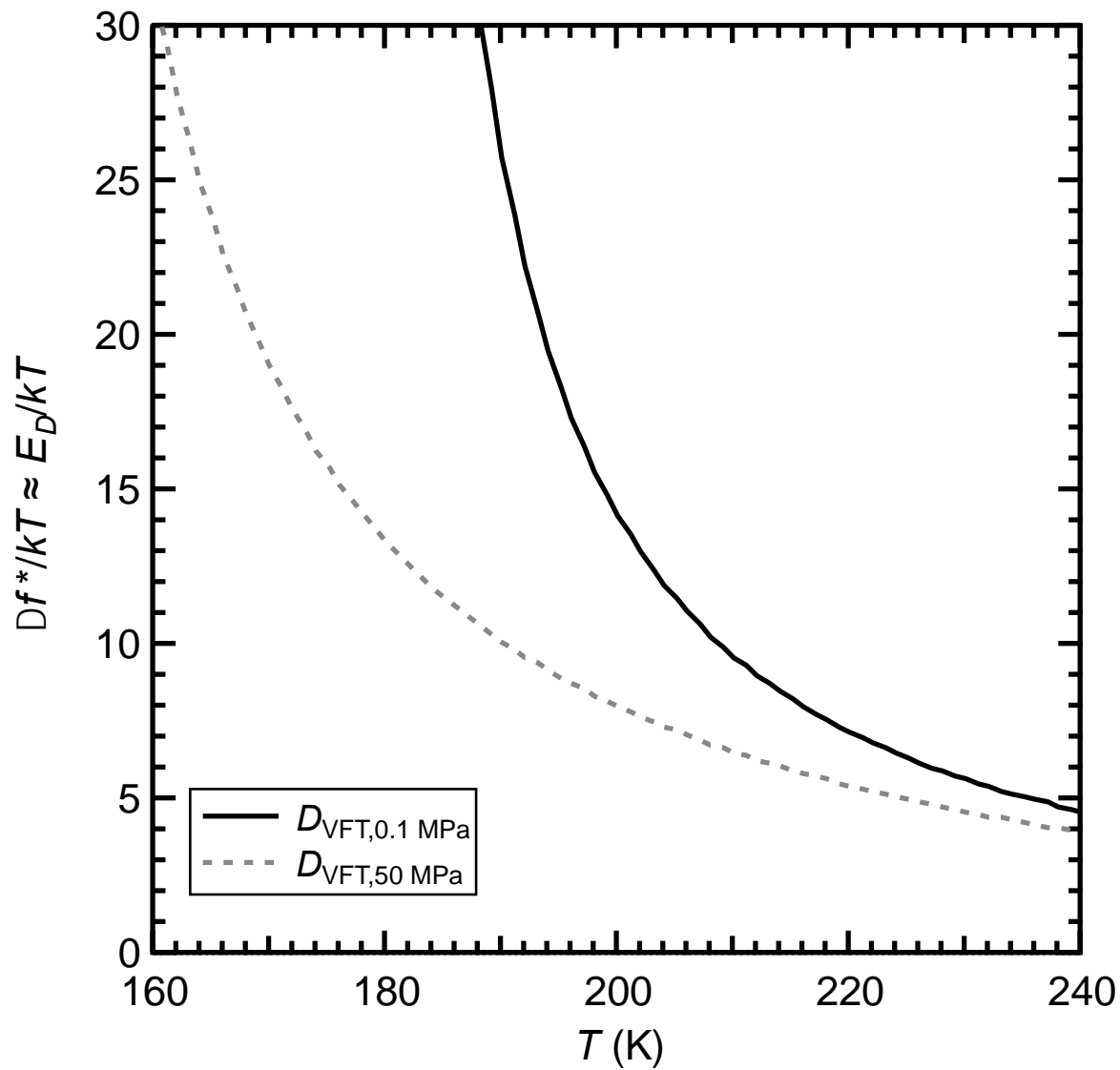


**Figure S3.** The kinetic barrier ( $\Delta f^*$ ) over a wide temperature range. The  $\Delta f^*$  at 0.1 MPa (black solid line) increases much faster than at 50 MPa (gray dashed line) with decreasing temperature.

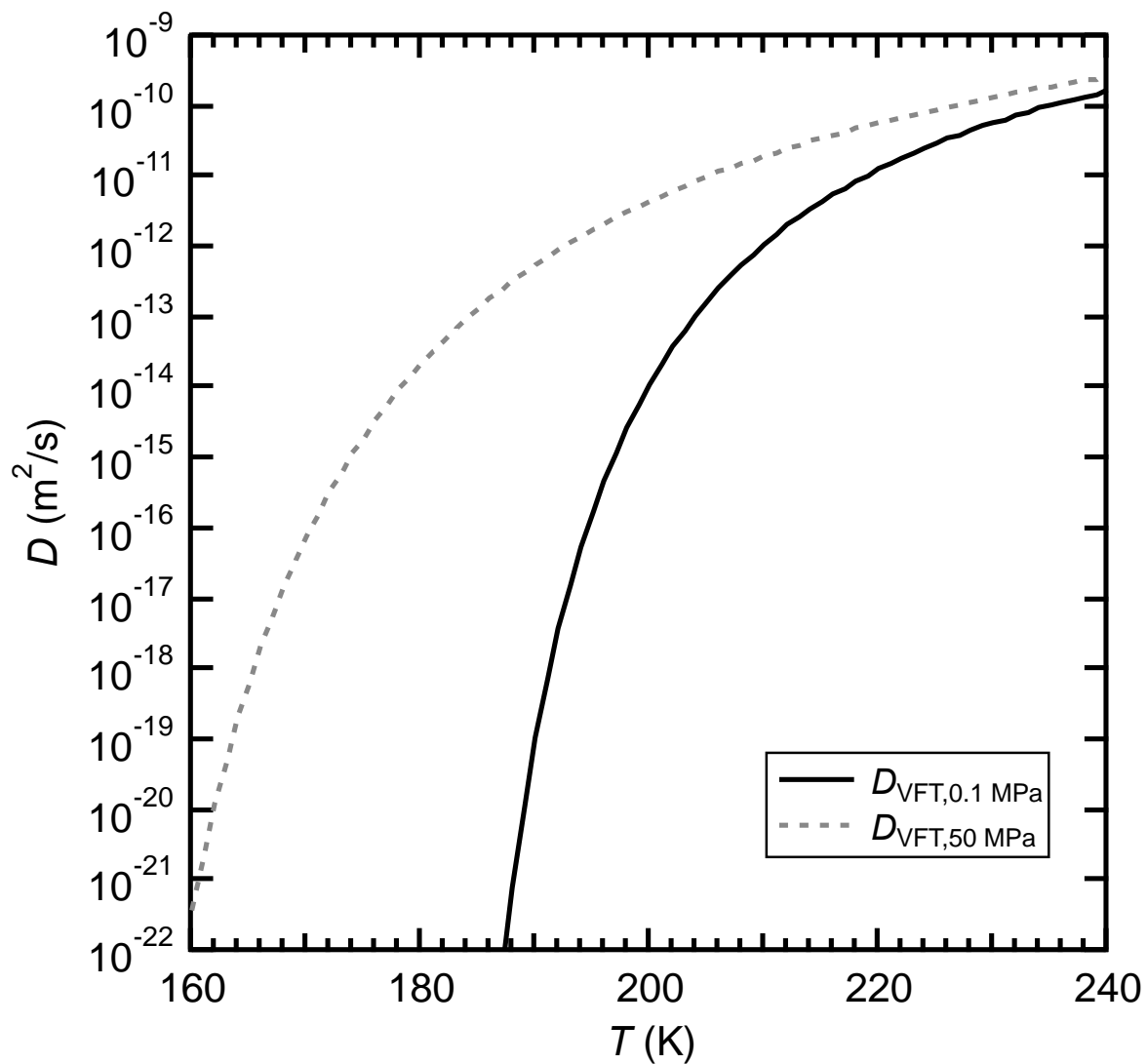


**Figure S4.** The diffusivity based on VFT fits to data of Prielmeier *et al.*<sup>13</sup> extrapolated to the “no-man’s land” region. The diffusivity at 50 MPa (gray dashed line) is much larger than at 0.1 MPa (black solid line), particularly below  $T_H$ .

**Tabulated experimental data and calculated ice nucleation rates.**

**Table S1.** A summary of experimental data collected as microdroplets evaporatively cool and freeze in vacuum. The distance represents distance between the nozzle exit and the interaction region where X-rays hit the droplet. The droplet diameters and speeds were adjusted to best fit experimentally determined droplet parameters from optical droplet measurements, volumetric liquid flow rates of the droplets, and droplet generation frequency.<sup>14</sup> The temperatures and their uncertainties are estimated from the Knudsen theory of evaporative cooling with a calibration made by comparing the liquid water wide-angle scattering signal in this experiment against larger droplets evaporating in vacuum and against synchrotron measurements of water in a cooling cell.<sup>14</sup> The ice fraction ( $f_{ice}$ ) represents the fraction of ice-containing shots at a particular distance with uncertainty that corresponds to the standard deviation of individual recordings collected at each distance and include variations in the hit rate and droplet trajectory jitter.

Distance (mm)	Temperature (K)	$f_{ice}$
Droplet diameter = 12.4 $\mu\text{m}$		
Droplet velocity = 10.35 m/s		
12.35	252 $^{+2}_{-1}$	0.001 $\pm$ 0.001
21.41	237 $^{+2}_{-0.2}$	0.001 $\pm$ 0.001
30.60	232 $^{+2}_{-0.1}$	0.001 $\pm$ 0.001
40.40	229 $^{+2}_{-1}$	0.181 $\pm$ 0.112
45.60	228 $^{+2}_{-1}$	0.836 $\pm$ 0.046
50.62	227 $^{+2}_{-1}$	0.971 $\pm$ 0.048
Droplet diameter = 8.7 $\mu\text{m}$		
Droplet velocity = 19.23 m/s		
25.88	233 $^{+2}_{-1}$	0.001 $\pm$ 0.001
36.04	230 $^{+2}_{-1}$	0.048 $\pm$ 0.006
46.09	228 $^{+2}_{-1}$	0.183 $\pm$ 0.051

**Table S2.** A summary of ice nucleation rate ( $J$ ) estimated from the measured  $f_{ice}$ . The nucleation rate uncertainty accounts for the standard deviation in  $f_{ice}$  and the uncertainty in the number of ice nuclei in each X-ray shot that shows Bragg reflections (see Experimental Section).

Distance (mm)	Temperature (K)	$J$ ( $\text{cm}^{-3} \text{s}^{-1}$ )
Droplet diameter = 12.4 $\mu\text{m}$		
Droplet velocity = 10.35 m/s		
35.50	230 $^{+2}_{-1}$	$2.11 \times 10^{11+3.12 \times 10^{12}}$ $-1.38 \times 10^{11}$
43.00	228 $^{+2}_{-1}$	$3.22 \times 10^{12+4.60 \times 10^{13}}$ $-7.90 \times 10^{11}$
48.12	227 $^{+2}_{-1}$	$3.58 \times 10^{12+5.76 \times 10^{13}}$ $-2.79 \times 10^{12}$
Droplet diameter = 8.7 $\mu\text{m}$		
Droplet velocity = 19.23 m/s		
30.96	232 $^{+2}_{-1}$	$2.69 \times 10^{11+3.81 \times 10^{12}}$ $-3.90 \times 10^{10}$
41.07	229 $^{+2}_{-1}$	$8.45 \times 10^{11+1.22 \times 10^{13}}$ $-3.71 \times 10^{11}$

## Thermophysical and transport properties of water.

**Table S3.** Thermophysical and transport properties of water.

Water		Refs.
<i>Molecular weight</i> (kg mol <sup>-1</sup> )		
$M$	$18.015 \times 10^{-3}$	
<i>Equilibrium vapor pressure</i> (Pa)		
Liquid, $p_{e,l}$	$\exp(54.842763 - 6763.22/T - 4.210\ln(T) + 0.000367T + \tanh(0.0415(T - 218.8)) \times (53.878 - 1331.22/T - 9.44523\ln(T) + 0.014025T))$	15
Hexagonal ice $I_h$ , $p_{e,lh}$	$\exp(9.550426 - 5723.265/T + 3.53068\ln(T) - 0.00728332T)$	15
Cubic ice $I_c$ , $p_{e,lc}$	$p_{e,lh} \exp(155/RT)$	7,15
<i>Liquid isothermal compressibility</i> (Pa <sup>-1</sup> )		
0.1 MPa, $\kappa_{T,0.1MPa}$	$\sim 10.0 \times 10^{-10}$ , at $T = 238$ K	16
50 MPa, $\kappa_{T,50MPa}$	$\sim 1.2 \times 10^{-10}$ , at $T = 200$ K	16
<i>Density</i> (kg m <sup>-3</sup> )		
Liquid, $\rho_l$	$(0.08\tanh((T - 225)/46.2) + 0.7415((647.15 - T)/647.15)^{0.33} + 0.32) \times 10^3$	10
Hexagonal ice $I_h$ , $\rho_{lh}$	$(-1.3103 \times 10^{-9} T^3 + 3.8109 \times 10^{-7} T^2 - 9.259 \times 10^{-5} T + 0.94040) \times 10^3$	15
Cubic ice $I_c$ , $\rho_{lc}$	$\rho_{lh}$	7
<i>Interfacial free energy</i> (J m <sup>-2</sup> )		
Vapor-liquid, $\sigma_{vl}$	$(111.63 - 0.13167T)/1000$	17
<i>Liquid diffusivity</i> (m <sup>2</sup> s <sup>-1</sup> )		
0.1 MPa, $D_{VFT,0.1MPa}$	$4.14 \times 10^{-8} \exp(-347/(T-177))$	13
50 MPa, $D_{VFT,50MPa}$	$8.90 \times 10^{-8} \exp(-563/(T-143))$	13
<b>CNT fit to microdroplets data (red line in Fig. 2a and 2b)</b>		
<i>Solid-liquid interfacial free energy</i> (J m <sup>-2</sup> )		
$\sigma_{sl}(T)$	$(20.8 \times (T/235.8)^{0.3})/1000$	7
<i>Liquid diffusivity</i> (m <sup>2</sup> s <sup>-1</sup> )		
$D(T) \sigma_{sl}$	$1.67 \times 10^{-8} \exp(5.698332 \times 10^{-2} T^2 - 2.728998 \times 10^1 T + 3.271878 \times 10^3)$	

**CNT for “fragile” liquid scenario (black dotted line in Fig. 2a and 2b)**

\*

*Solid-liquid interfacial free energy* (J m<sup>-2</sup>)

$$\sigma_{sl}(T) = (20.8 \times (T/235.8)^{0.67})/1000$$

*Liquid diffusivity* (m<sup>2</sup> s<sup>-1</sup>)

$$D(T) = kT/(6\pi\eta r)$$

\*\*

where

$$r = (3M/(4\rho\pi N_A))^{1/3}$$

$$N_A = 6.022 \times 10^{23}$$

$$k = 1.3806 \times 10^{-23}$$

$$\eta = \eta_0 \exp(\eta_D T_0 / (T - T_0))$$

$$\eta_0 = 10^{12}$$

$$\eta_D = 7$$

$$T_0 = T_g / (1 + 7 / (\ln(10) \log(17)))$$

$$T_g = 136$$

**CNT scenario with  $\Delta F_{p=0.1\text{MPa}}^*$ ,  $D_{\text{VFT},0.1\text{MPa}}$**

*Solid-liquid interfacial free energy* (J m<sup>-2</sup>)

$$\sigma_{sl}(T) = (20.8 \times (T/235.8)^{0.67})/1000$$

*Liquid diffusivity* (m<sup>2</sup> s<sup>-1</sup>)

$$D(T) = D_{\text{VFT},0.1\text{MPa}}$$

13

**CNT scenario with  $\Delta F_{p=50\text{MPa}}^*$ ,  $D_{\text{VFT},0.1\text{MPa}}$**

*Solid-liquid interfacial free energy* (J m<sup>-2</sup>)

$$\sigma_{sl}(T) = (20.8 \times (T/235.8)^{0.67})/1000$$

*Liquid diffusivity* (m<sup>2</sup> s<sup>-1</sup>)

$$D(T) = D_{\text{VFT},0.1\text{MPa}}$$

13

**CNT scenario with  $\Delta F_{p=50\text{MPa}}^*$ ,  $D_{\text{VFT},50\text{MPa}}$**

*Solid-liquid interfacial free energy* (J m<sup>-2</sup>)

$$\sigma_{sl}(T) = (20.8 \times (T/235.8)^{0.67})/1000$$

*Liquid diffusivity* (m<sup>2</sup> s<sup>-1</sup>)

$$D(T) = D_{\text{VFT},50\text{MPa}}$$

13

\*We follow Jenniskens and Blake<sup>18</sup> to estimate the “fragile” liquid nucleation rate from CNT. However, here we used diffusivity in the CNT formulation.

\*\* The diffusivity is estimated from viscosity using Stokes-Einstein relationship. We follow Jenniskens and Blake<sup>18</sup> to describe the viscosity over a wide range of temperature using VFT law.

## REFERENCES

- (1) Debenedetti, P. G. *Metastable Liquids: Concepts and Principles*; Princeton University Press: Princeton, 1997.
- (2) Frenkel, J. *Kinetic Theory of Liquids*; Oxford University Press: Oxford, 1946.
- (3) Němec, T. Estimation of Ice–water Interfacial Energy Based on Pressure-Dependent Formulation of Classical Nucleation Theory. *Chem. Phys. Lett.* **2013**, *583*, 64–68.
- (4) Turnbull, D.; Fisher, J. C. Rate of Nucleation in Condensed Systems. *J. Chem. Phys.* **1949**, *17*, 71–73.
- (5) Murray, B. J.; O’Sullivan, D.; Atkinson, J. D.; Webb, M. E. Ice Nucleation by Particles Immersed in Supercooled Cloud Droplets. *Chem. Soc. Rev.* **2012**, *41*, 6519–6554.
- (6) Chushak, Y.; Bartell, L. S. Crystal Nucleation and Growth in Large Clusters of SeF<sub>6</sub> from Molecular Dynamics Simulations. *J. Phys. Chem. A* **2000**, *104*, 9328–9336.
- (7) Murray, B. J.; Broadley, S. L.; Wilson, T. W.; Bull, S. J.; Wills, R. H.; Christenson, H. K.; Murray, E. J. Kinetics of the Homogeneous Freezing of Water. *Phys. Chem. Chem. Phys.* **2010**, *12*, 10380–10387.
- (8) Bartell, L. S.; Dibble, T. S. Electron Diffraction Studies of the Kinetics of Phase Changes in Molecular Clusters: Freezing of Carbon Tetrachloride in Supersonic Flow. *J. Phys. Chem.* **1991**, *95*, 1159–1167.
- (9) Jeffery, C. A.; Austin, P. H. Homogeneous Nucleation of Supercooled water: Results from a New Equation of State. *J. Geophys. Res.* **1997**, *102*, 25269–25279.
- (10) Manka, A.; Pathak, H.; Tanimura, S.; Wölk, J.; Strey, R.; Wyslouzil, B. E. Freezing Water in No-Man’s Land. *Phys. Chem. Chem. Phys.* **2012**, *14*, 4505–4516.
- (11) Bhabhe, A.; Pathak, H.; Wyslouzil, B. E. Freezing of Heavy Water (D<sub>2</sub>O) Nanodroplets. *J. Phys. Chem. A* **2013**, *117*, 5472–5482.
- (12) Stan, C. A.; Schneider, G. F.; Shevkoplyas, S. S.; Hashimoto, M.; Ibanescu, M.; Wiley, B. J.; Whitesides, G. M. A Microfluidic Apparatus for the Study of Ice Nucleation in Supercooled Water Drops. *Lab Chip* **2009**, *9*, 2293–2305.
- (13) Prielmeier, F. X.; Lang, E. W.; Speedy, R. J.; Lüdemann, H.-D. The Pressure Dependence of Self-Diffusion in Supercooled Light and Heavy Water. *Berichte der Bunsengesellschaft für Phys. Chemie* **1988**, *92*, 1111–1117.

- (14) Sellberg, J. A.; Huang, C.; McQueen, T. A.; Loh, N. D.; Laksmono, H.; Schlesinger, D.; Sierra, R. G.; Nordlund, D.; Hampton, C. Y.; Starodub, D.; et al. Ultrafast X-Ray Probing of Water Structure below the Homogeneous Ice Nucleation Temperature. *Nature* **2014**, *510*, 381–384.
- (15) Murphy, D. M.; Koop, T. Review of the Vapour Pressures of Ice and Supercooled Water for Atmospheric Applications. *Q. J. R. Meteorol. Soc.* **2005**, *131*, 1539–1565.
- (16) Holten, V.; Anisimov, M. A. Entropy-Driven Liquid-Liquid Separation in Supercooled Water. *Sci. Rep.* **2012**, *2*, 713.
- (17) Huang, J.; Bartell, L. S. Kinetics of Homogeneous Nucleation in the Freezing of Large Water Clusters. *J. Phys. Chem.* **1995**, *99*, 3924–3931.
- (18) Jenniskens, P.; Blake, D. F. Crystallization of Amorphous Water Ice in the Solar System. *Astrophys. J.* **1996**, *473*, 1104–1113.